IMPACT: International Journal of Research in Engineering & Technology (IMPACT: IJRET)
ISSN(E): 2321-8843; ISSN(P): 2347-4599
Vol. 2, Issue 4, Apr 2014, 217-232

BEARING CAPACITY OF FOOTING ON SLOPPING ANISOTROPIC ROCK MASS

D K SHUKLA[1], MAHENDRA SINGH[2] & K K JAIN[3]

[1,3]Department of Civil Engineering, Jaypee University of Engineering and Technology, Raghogarh, Madhya Pradesh, India

[2]Department of Civil Engineering, Indian Institute of Technology, Roorkee, Uttarakhand, India

ABSTRACT

Rocks are inherently strong and stable to withstand loads. Rock mass bearing capacity governs by its discontinuities like folds, faults, bedding plane which could be assessed by various theories considering rock mass either isotropic or anisotrpic medium. Despite having strong and stable behavior, a jointed rock mass under unconfined condition has very low bearing capacity, sometimes rock mass collapse under its own weight. In this study, bearing capacity of jointed rock mass has been assessed under unconfined condition. The bearing capacity of footing at the edge of slopping anisotropic rock mass has been obtained experimentally in plane strain condition. The jointed rock mass assembled using sand stone element of 25 mm × 25 mm × 75 mm along different joint angles of 15˚,30˚,45˚,60˚,75˚ and 90˚ and slope angles of 30˚,45˚,60˚,75˚, and 90˚ with the horizontal. All the tests were performed on stable rock mass having continuous joint angle. It is observed that magnitude of load intensity at failure on slope depends upon joint angle with major principal axis, joint frequency, joint strength, unconfined compressive strength and modulus of elasticity of rock mass and mode of failure. Joint angle and modes of failure are important parameters, which govern the load intensity at slope. Load carrying capacity of rock mass can be assessed more rationally if the mode of failure can be predicted. The mode failures as observed are buckling/sliding/rotation/toppling towards unconfined side. Analysis of the experimental data has been attempted based on Caver's (1981) suggestions and Euler's theory. Comparative values of failure loads have been predicted

KEYWORDS: Bearing Capacity, Slopping Anisotropic Rock Mass, Plain Strain, Failure Modes, Rock Mass Buckling

INTRODUCTION

Rock mass consists of intact rock separated by geological discontinuities such as joints, faults and bedding planes. The rock mass behavior is generally governed by the interaction of intact blocks with these discontinuities under an applied load. The presence of weak planes, joints and other discontinuities make the strata weak and the correct assessment of its load bearing capacity for constructing any major structure on the rock mass becomes complex. A foundation on rock, therefore, should be designed with as much care as a foundation on soil. Most of the methods available for finding the ultimate bearing capacity of jointed rock mass consider the mass an isotropic medium [8, 9]. The applicability of these methods to rock masses remains doubtful. Methodologies suggested for jointed rock mass are those proposed by the Hoek-Brown failure criterion for rocks and rock masses are most widely used non-linear criterion world over. Anisotropic rock mass bearing capacity given by Ramamurthy and Arora predicted on the basis of joint factor, Singh and Rao, predicted on the basis of Bell's approach using joint factor [11]. All the methods mentioned above give reasonably good results for confined rock mass. However, these theories are not suitably applicable for unconfined rock mass.

The bearing capacity of rock mass at slope usually assessed by empirical equations [5], design charts [2], limiting equilibrium method or plasticity equations [9.12]. Jointed rock mass bearing capacity in confined and unconfined condition could be assessed accurately only after determination of uniaxial compressive strength ($\boldsymbol{\sigma}_{cj}$), modulus of elasticity of rock mass, angle of joint plane with loading direction, type of failure and other rock mass properties Adhikary et al.(2001) devised on large deformation model of rock masses with elastic layers of equal mechanical properties and equal thickness on the basis of Cosserat continuum theory in to finite element code. A design chart given by them suitable for assessing the stability of foliated rock slopes in dry state. Pore water as well as cross jointing in not considered by Adhikaryet al. (2001) Stability analysis and stabilisation of toppling failure by Mehdi Amini et. al. (2009) presented an analytical method for the determination of the magnitude and point of application of inter column forces in rock mass with a potential of flexural buckling. A simple approach to analyse buckling of a rock slope was presented by Cavers (1981) considered flexural buckling of plane slab, three hinges buckling of plane and curve slopes.

In the present study, bearing capacity at slope edge has been assessed by experimental verification with the objective to find out the resistance to failure is given by rock mass and the modes of failure. Experiments were conducted on anisotropic rock mass in plane strain condition. Experimental results have been compared with analytical results obtained on the basis of mode of failure.

Though the natural configuration of jointed rock mass in the field is not possible to generate in the laboratory, sand stone elements of size 25 mm × 25 mm × 75 mm is used to assemble jointed rock mass. So far only artificial material has been used by researchers. Experiments were conducted in a specially designed and fabricated bearing capacity test apparatus of 200 ton capacity. The rock mass model dimensions 750 mm × 750 mm ×150 mm are considered large enough to nullify the scale effect.

LITERATURE REVIEW: ROCK MASS BEARING CAPACITY THEORIES

Hoek-Brown Failure Criteria for Rock Masses

The Hoek-Brown failure criterion for rocks and rock masses is the most widely used non-linear criterion world over. It was originally suggested in Hoek E.1980 [5] and subsequently updated in Hoek E, Brown E T(1988)[7], Hoek E, and BrownE T. (1997)[8], Hoek, E.(2000)[9], Hoek E, Carranza-Torres C, and Corkum B. (2002) [10], Hoek E, Marinos P, and Marinos V (2005) [11], respectively by incorporating the experience gained by the authors and other researchers in using the criterion.

Cavers D S (1881)

Cavers (1981) [6] predicted buckling modes of failure are a possibility whenever a continuous joints approximately parallel to the slope, separates a thin slab. The maximum load that can be carried per unit width, before buckling takes place, is as given by Cavers (1981) [6] for flexural buckling of plane slabs by classical buckling theory.

$$\frac{\boldsymbol{P_{cr}}}{\boldsymbol{B}} = \frac{\boldsymbol{K\pi^2 E_j I}}{\boldsymbol{B L_b^2}} \tag{1}$$

Application of Eulers formula for a slope requires additional assumptions for buckling length. According to Cavers (1981), the driving force given as

$$P_D = (W_D \sin\alpha - W_D \cos\alpha \tan\phi_j - l_D C)b \tag{2}$$

These results should form upper and lower bound on l_b/l for the conditions and material used. For rock $l_b/l = 0.5$ and substituting the slab dimensions and unit weight (γ) in equation (2) becomes as

$$\frac{P_D}{b} = 0.75ld\left(\gamma \sin\alpha - \gamma \cos\alpha \tan\phi_j - C/d\right) \tag{3}$$

Ramamurthy and Arora (1994)

Arora (1987) [3] and Ramamurthy and Arora (1994) [4] provided solution for determination of uncofined compresive strength through concept of joint factor. They give maximum importance to joint frequency, joint inclination and joint strength for predicting behaviour of jointed rocks. By clubbing these three parameters, a factor called Joint Factor (J_f) was been defined as.

$$J_f = \frac{J_n}{nr} \tag{4}$$

Where, J_n = Number of joints per meter in the direction of major principal stress,

n = Inclination factor which depends on orientation of joint with respect to loading direction,

r= Joint strength parameter $=\sigma_{cj} / \sigma_{ci} = \tan \O_j$

$\O_j$ = Discontinuity friction angle

The value of J_f thus obtained is an indicative of how much weakness has been brought to intact rock by presence of joints. The value of 'n' is given in the table 1. Values of 'r' have to be determined by conducting direct shear test.

Table 1: Values of Inclination Parameter, n for Different Joint Orientation, β° from Ramamurthy and Arora (1994)

Orientation of Joint (βo)	0	10	20	30	40	50	60	70	80	90
Inclination parameter (n)	0.814	0.460	0.105	0.046	0.071	0.306	0.465	0.634	0.814	1.000

The average value of strength of the jointed rock mass is the unconfined compressive strength of the jointed rock mass that is given as

$$q_u = \sigma_{cj} = \sigma_{ci} \exp\left(-0.008 J_f\right) \tag{5}$$

Singh and Rao (2005)

Singh and Rao (2005) [18] suggested a procedure to estimate the ultimate bearing capacity of shallow foundation in anisotropic rock masses. The approach considers the strength properties of the mass as a whole, which depends both on joint properties and intact rock properties. Bell‟s approach has been used for computing bearing capacity, in which the ultimate bearing capacity is determined as a major principal stress at failure under confining pressure acting on the mass beneath a smooth foundation. To define the strength of the rock mass, a simple parabolic equation derived based on critical state of rock has been used. The uniaxial compressive strength of jointed rock mass, which is an input parameter to the strength criterion, is determined using the Joint Factor concept. As per this approach, the active and passive zones develop in the rock mass under a smooth strip footing. It is assumed that these zones are divided by a vertical line passing through the edge of the footing. The length of the strip footing is assumed to be infinite and the ground surface is horizontal. The rock mass under the footing, as well as the adjacent mass, is assumed to be in a triaxial stress state. The major principal stress for the active zone just beneath the footing, acts in vertical direction. For the passive zone, the major principal stress acts in the horizontal direction and the effective surcharge acts as the minor principal stress. At the time of failure, equilibrium of two adjacent elements of rock prisms is considered, one just beneath the edge of the footing (Element II) and the other just outside (element I) figure 1.

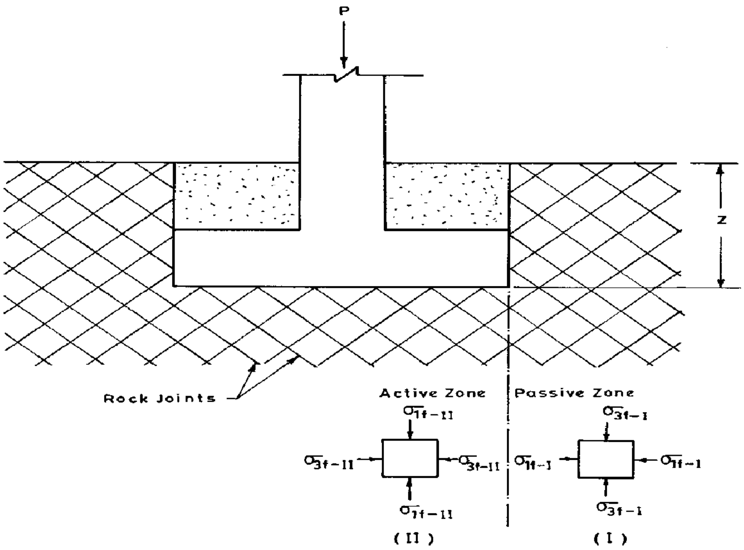

Figure 1: Bearing Capacity Test Apparatus (J0090SL45)

For element-I (adjacent element), at the time of failure:

$$\sigma_{3-1} = \gamma z \ and \ \sigma_{1-1} = f(\sigma_{3-1}) \quad (6)$$

where γ = unit weight of the rock mass,

z = depth of the foundation,

$\sigma_{3\text{-I}}$ = confining stress acting on element I at the time of failure and

$\sigma_{1\text{-I}}$ = major principal stress at element I at the time of failure.

For element II (element below the footing), at the time of failure:

$\sigma_{3\text{-II}}$ = confining stress = $\sigma_{1\text{-I}}$

σ 1-II = major principal stress for element II at the time of failure,

The ultimate bearing capacity is given as:

$$q_{ult} = \sigma_{1-II} \quad (7)$$

The uniaxial compressive strength σ_{cj} depends on the Joint Factor J_f and the mode of failure (Singh et al., 2002). Its value is estimated as:

$$\sigma_{cj} = \sigma_{ci} \exp\left(aJ_f\right) \quad (8)$$

where a is an empirical coefficient depending on failure mode as presented in Table 2

Table 2: Coefficient 'a' for Estimating σ_{cj}

Failure Mode	Coefficient "a"
Splitting/ Shearing	- 0.0123
Sliding	-0.0180
Rotation	-0.0250

The strength may be computed for these extreme values, and for intermediate values of σ, linear interpolation can be made.

Modulus of Jointed Rocks

Ramamurthy and Arora 1993[4], The ratio of moduli of jointed rock and that of the intact rock in uniaxial compression was linked to the joint factor

$$E_r = \frac{E_j}{E_i} = \exp\left(-1.15 \times 10^{-2} J_f\right) \tag{9}$$

Experimental Details

Figure 2: Bearing Capacity Test Apparatus (J0090SL45)

Carefully planned specific experimental program was executed to achieve the objective of the study. A 200 ton bearing capacity test apparatus shown in the figure 2 for testing the rock mass in plane strain conditions is designed and fabricated. The vertical load observed by proving ring placed over jack and vertical displacement was recorded at all four corner of footing during testing of the specimen up to failure. Perspex transparent sheet is fixed on the front side to observe the failure pattern; Steel plates were fixed on the other two sides. Approximately 2000 to 2400 number of blocks were required to form one blocky mass.

Element joint angle was varied from 0°,15° 30° 45° 60° 75° to 90° whereas side slope inclination also varied 90º, 75°,60°,45° and 30° with horizontal. For side slope 15˚ experiments were not conducted because it approached almost flat. 150 mm × 150 mm footing was placed exactly on the edge of the rock mass. An experiment is designated as J0090SL45 which indicates that joint set-1angle (θ_1) is 00˚ with the horizontal and joint set-2 angle (θ_2) 90˚ and side slope angle (α) 45˚ as shown in figure 3. The size of the rock mass specimen was kept as 750 mm x 750 mm x 150 mm while the size of elemental blocks used was 25 mm x 25 mm x 75 mm.

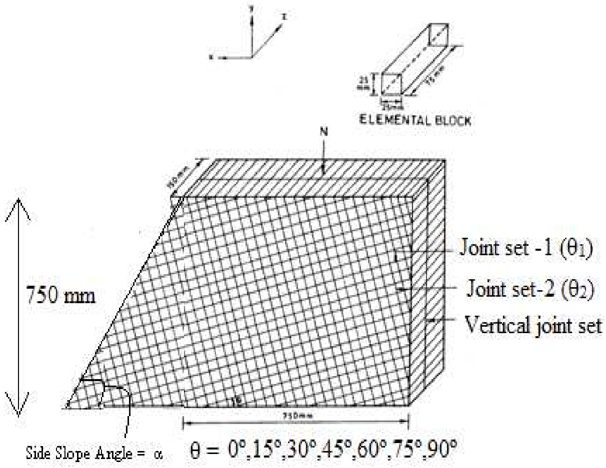

Figure 3: Rock Mass Arrangements with Variation in Joint Set Angle and Side Slope

Model Material

Sand stone is used to make the elements as model material. Physical and the engineering properties of the model material are presented in Table 3. These properties are obtained as per Indian standard procedure using code as IS 9221-1979, IS-10082-1982, IS-13030-1991. Average uniaxial compressive strength of the intact material has been found to be 48.5 MPa. Failure strain of the intact material has been found to be 0.81 % and the tangent modulus obtained at 50% of failure stress was observed to be 8773 MPa. The modulus ratio, Et50/σci, of the material is found to be 181.

The value of basic friction angle of joint (φj) was found as 29º by direct shear test. Shear strength parameters for intact material (ci and φi) were obtained by conducting triaxial tests under varying confining pressures i.e. at σ_3 = 2.45 MPa, 4.9MPa 7.35 MPa and 14.7 MPa respectively.

Table 3: Physical and Engineering Properties of the Model Material

S No	Property	Value
1	Dry unit weight, γd (kN/m^3)	24.91
2	Specific gravity, G	2.52
3	Uniaxial Compressive Strength, σ_{ci} (MPa)	48.5
4	Failure strain, ε_f (%)	0.81
5	Tangent modulus, E_{t50} (MPa)	8773
6	Tangent modulus, E (MPa)	5820
7	Brazilian strength, σ_t (kN)	15.8
8	Friction angle of joint, φ_j (degree)	30
9	Friction angle of intact model material, φ_i (degree)	39
10	Cohesion of intact model material, c_i (MPa)	19

EXPERIMENTAL RESULTS AND OBSERVATION

Experiments are conducted by placing the footing placed at edge of the slope. Failure load and deformation at all four corners of the footing is measured. The mode of failure was observed either bucklingor a combination of buckiling and sliding failure in most of the tests. For joint angle 00º- 90º and joint 15-75 buckiling failure observed. Whereas for joint 30º-60º, 45º-45º and 60º-30º sliding and buckling observed. Load intensities were 20-100 times less than its unconfined compressive strength. Experimental results have shown in table 4 below.

Joint Angle 00º-90º (J0090)

A zone of compression has been observed with vertical joints opened up just below footing. Vertical joints opening commenced from centre of footing towards unconfined side. Finally buckling failure takes place (figure 4 to figure 8). Average footing settlement observed as minimum 1.71 mm for the side slope 90º and maximum 4.58 mm for the side slope 30º respectively. Load intensities were as low as 1.39 MPa for the side slope 90 and maximum 2.92 MPa for the side slope 30º. Experimental results shows footing settlement and load intensity increases with decrease in side slope angle with horizontal.

Figure 4: At Failure for the Test J0090SL90

Figure 5: At Failure for the Test J0090SL75

Figure 6: At Failure for the Test J0090SL60

Figure 7: At Failure for the Test J0090SL45

Figure 8: At Failure for the Test J0090SL30

Joint Angle 15º-75º (J1575)

A little zone of compression has been observed with vertical joints opened up just below footing in the direction of vertical plane. Side slope 90º with joint angle 15º-75º (J1575SL90) gave zero load intensity because elements sliced by its own weight. Similarly, Vertical joints opening commenced from centre of footing towards unconfined side. Finally buckling failure takes place (figure 9 to figure 12). Average footing settlement observed as minimum 4.15 mm for the side slope 60º and maximum 11.2 mm for the side slope 45º. Load intensities were as low as 0 MPa for the side slope 90 and maximum 2.92 MPa for the side slope 30º.

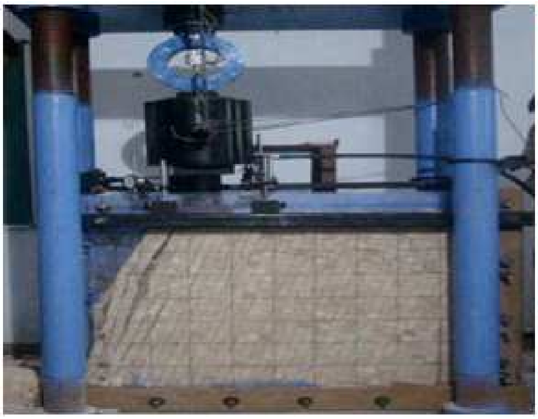

Figure 9: At Failure for the Test J1575SL75

Figure 10: At Failure for the Test J1575SL60

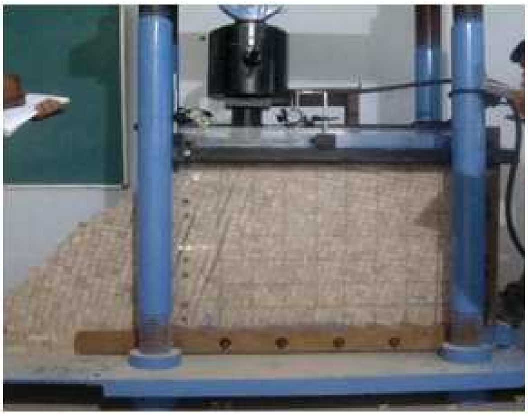

Figure 11: At Failure for the Test J1575SL45

Figure 12: At Failure for the Test J1575SL30

Joint Angle 30º-60º (J3060)

No zone compression observed below the base footing. In the beginning as the load applied elements below the base of footing sliced in the direction of joint angle (figure 13 to figure 15). The magnitude of load intensities were governs by toe resistance (Toe support is provided). Finally vertical joints opened up and buckling takes. Load intensities were negligible in sliding (toe support not provided). Average footing settlement observed as minimum 3.69 mm for the side slope 60º and maximum 8.63mm for the side slope 45º. Load intensities were as low as 0 MPa for the side slope 90º and 75º and maximum 1.06 MPa for the side slope 30º.

Figure 13: At Failure for the Test J3060SL60 **Figure 14: At Failure for the Test J3060SL45**

Joint Angle 45º-45º (J4545)

No zone compression observed below the base footing. In the beginning as the load applied elements below the base of footing sliced in the direction of joint angle (figure 16 to figure 17). The magnitude of load intensities were governs by toe resistance (Toe support is provided). Finally vertical joints opened up and buckling takes. Load intensities were negligible in sliding (toe support not provided). Average footing settlement observed as minimum 9.88 mm for the side slope 45º and maximum 10.66 mm for the side slope 30º. Load intensities were as low as 0 MPa for the side slope 90º, 75º, 60º and maximum 0.63 MPa for the side slope 30º.

Figure 15: **At failure for the Test J3060SL45** **Figure 16: At failure for the Test J4545SL4**5

Figure 17: At failure for the Test J4545SL30 **Figure 18: At Failure for the Test J3060SL30**

Joint Angle 60º-30º (J6030)

No zone compression observed below the base footing. In the beginning as the load applied elements below the base of footing sliced in the direction of joint angle figure 18. At failure momentarily buckling takes place towards unconfined side. Load intensities were as low as 0 MPa for the side slope 90º, 75º, 60º, 45º and maximum 0.19 MPa for the side slope 30º.

Table 4: Experimental Results

S No	Test	Load Intensity (MPa)	Average Settlement (mm)	**Buckling Length (mm)
1	J0090-SL90	1.39	1.75	675
2	J0090-SL75	2.92	2.95	625
3	J0090-SL60	2.81	2.86	625
4	J0090-SL45	2.82	3.27	625
5	J0090-SL30	2.92	4.58	675
6	J1575-SL90	0	0	0
7	J1575-SL75	1.17	4.63	750
8	J1575-SL60	1.94	4.15	675
9	J1575-SL45	2.59	11.20	650
10	J1575-SL30	2.92	7.88	625
11	J3060-SL90	0	0	0
12	J3060-SL75	0	0	0
13	J3060-SL60	0.52	3.69	875
14	J3060-SL45	0.52	8.63	850
15	J3060-SL30	1.06	4.25	850
16	J4545-SL90	0	0	0
17	J4545-SL75	0	0	0
18	J4545-SL60	0	0	0
19	J4545-SL45	0.52	9.88	1075**
20	J4545-SL30	0.63	10.66	1075**
21	J6030-SL90	0	0	0
22	J6030-SL75	0	0	0
23	J6030-SL60	0	0	0
24	J6030-SL45	0	0	0
25	J6030-SL30	0.19	5.06	1500**

Note: * Settlement recorded at all four corner of footing. Average of all four dial gauge readings are given
** Buckling Length L_b is measured on the basis of rock specimens shifted from its original position at failure
*** A combination of sliding and buckling failure occurred than entire slope length taken as buckling length

ANALYSIS OF RESULTS

Experimental results analysed for load intensities by classical buckling theory (Euler's method) because at failure buckling takes place. As per classical buckling theory it is assumed that column is straight, weightless, elastic and obeys Hook's law. Load intensity has been calculated by Eulers's method for straight column because Euler's theory for inclined column gives 100-500 times less load intensity as compare to experimental value. As observed from experiments either buckling or sliding take place at failure. For the analysis of results buckling length has been observed from pictures / video taken at the time experiments at failure. In the case of a combination of sliding and buckling failure takes place then entire slope length is considered as buckling length because if rock mass is free to slide then sliding take place or if rock mass restricted at toe then buckling will take place from toe. Analytical results have been given in table 5.

Table 5: Comparison of Buckling Load Intensity, Calculated and Experimental Results

S No	Test	P_{cr}	Calculated Load Intensity (MPa)	Experimental (MPa)	Corrected** Load Intensity (MPa)
1	J0090-SL90	6086.06	1.86	1.39	1.86
2	J0090-SL75	7571.56	2.17	2.92	2.17
3	J0090-SL60	8189.40	2.17	2.81	2.17
4	J0090-SL45	7571.56	2.17	2.82	2.17
5	J0090-SL30	7021.09	1.86	2.92	1.86
6	J1575-SL90	0	0	0	0
7	J1575-SL75	5687.09	1.52	1.17	1.45
8	J1575-SL60	7021.09	1.87	1.94	1.80
9	J1575-SL45	7571.56	2.02	2.59	1.94
10	J1575-SL30	8189.40	2.17	2.92	2.09
11	J3060-SL90	0	0	0	0
12	J3060-SL75	0	0	0	0
13	J3060-SL60	4178.27	1.11	0.52	0.96
14	J3060-SL45	4427.66	1.18	0.52	1.02
15	J3060-SL30	4427.66	1.18	1.06	1.02
16	J4545-SL90	0	0	0	0
17	J4545-SL75	0	0	0	0
18	J4545-SL60	0	0	0	0
19	J4545-SL45	2768.19	0.74	0.52	0.52
20	J4545-SL30	2768.19	0.74	0.63	0.52
21	J6030-SL90	0	0	0	0
22	J6030-SL75	0	0	0	0
23	J6030-SL60	0	0	0	0
24	J6030-SL45	0	0	0	0
25	J6030-SL30	1421.77	0.38	0.19	0.19

*Buckling Length L_b is measured on the basis of rock specimens shifted from its original position at failure.
**Calculated load intensity is resolved in vertical direction according to joint angle.
***In case of sliding and buckling occurred simultaneously than entire slope length taken as buckling length

A sample calculationfor experiment J0090SL30 analysed for load intensity as per buckling load method and J4545SL45 for sliding as well as buckling load method as given below.

Load Intensity for Experiment J0090SL30

Modulus of elasticity of rock masses calculated according to Ramamurthy & Rao theory.

J_n = 40 (one element size is 25 mm)

n = 0.814 (Table 1, Ramamurthy and Arora (1994)

Joint strength parameter (r) = $\tan\phi_j$ = 0.577

$$J_f = J_n/nr = 84.5 \tag{10}$$

Puting the value of J_f in equation- 9 and Modulus of elasticity (E_{t50}) of intact rock from table 3, we have

$$E_r = \frac{E_j}{E_i} = \exp\left(-1.15 \times 10^{-2} J_f\right) \tag{11}$$

E_j = 3319.05 MPa

The buckling load carrying capacity of footing can be calculated using equation-7 we have,

$$\frac{P_{cr}}{B} = \frac{K\pi^2 E_j I}{B L_b^2}$$

Where buckling length L_b = 675 mm taken from figure 8

E_j = 3319.05 MPa from equation-11

Moment of Inertia = $bd^3/12$, where

B = 15 cm d = 2.5 cm.

I = 19.53 cm^4

Hence we have

P_{cr} = 14042.22 × 3 N (Load is acting at the centre of footing which resulted effective buckling in three rock mass columns out of six)

Load Intensity = 42126.66/22500

=1.87 Mpa

Eulers theory P_{cr} = 1.87 < 2.92 MPa (Experimental Value).

Load Intensity for Experiment J4545SL45 for Inclined Column

J4545SL45 driving resistance due to inclined column, assuming cohesion negligible, according Cavers (1981) given as:

$$P_D = (W_D \sin\alpha - W_D \cos\alpha \tan\phi_j - l_D C)b$$

Weight of slab W_D calculated as:

Weight of one element = $0.025^3 \times 24.01$

= 1.1676×10^{-3} kN

Total elements in one column is 42 therefore weight of one column at slope 0.049 kN. Total six number of column below footing, so weight of slab W_D = 0.59kN

$\alpha = 45^\circ$

P_D = 0.00117MPa (Which is approximately 450 times less than experimental value)

Load Intensity for Experiment J4545SL45 for Vertical Column

If the same test analysed according to buckling of straight column we have

J_n = 40 (one element size is 25 mm)

n = 0.82 (Table 1, Ramamurthy and Arora 1994)

Joint strength parameter (r) = $\tan\phi_j$ = 0.577

$J_f = J_n/nr$ = 84.5

Puting the value of J_f from equation 10 and Modulus of elasticity (E_{t50}) of intact rock from table 3, we have

$$E_r = \frac{E_j}{E_i} = \exp\left(-1.15 \times 10^{-2} J_f\right)$$

E_j = 3319.05 MPa

The buckling load carrying capacity of footing can be calculated using equation-7 we have,

$$\frac{P_{cr}}{B} = \frac{K\pi^2 E_j I}{B L_b^2}$$

Where buckiling length L_b = 1075 mm (Entire slope length as shown in figure 16)

E_j = 3319.05 MPa

Moment of Inertia = $bd^3/12$, where

B = 15 cm d = 2.5 cm.

I = 19.53 cm^4

Hence we have

P_{cr} = 5536.39 × 3 N (Load is acting at the centre of footing which resulted effective buckling in three rock mass columns out of six)

Load Intensity = 42126.66/22500 = 0.74 MPa

Corrected for vertical load = 0.74 *cos* (45)= 0.52 MPa

Eulers theory P_{cr} = 0.52 < 0.54 MPa (Experimental Value).

As shown above that Euler's buckling analysis reasonably match the experimental data.

CONCLUSIONS

Bearing capacity of unconfined rock mass with continuous joints at slope edge analysed by Euler's method of buckling (vertical or inclined column) rationally. Bearing capacity of jointed rock mass is half of the total buckling load capcity when footing placed at edge of the slope because buckling was observed in three columns of unconfined side out of six columns of rock mass below the base footing. Average settlement of footing for joint angle (θ) = 0˚, 15˚, 30˚ (Buckling mode of failure) are less than the joint angle (θ) = 45˚, 60˚(Combination of Sliding and buckling mode of failure) due to mode of failure. Similarly the magnitude of bearing capacity is more for joint angle (θ) = 0˚, 15˚, 30˚(Buckling mode of failure)as compare to the joint angle (θ) = 45˚, 60˚(Combination of Sliding and buckling failure). Therefore it could conclude that buckling resistance alwaya greater than sliding resistance for continuous jointed rock mass.

ACKNOWLEDGEMENTS

The authors are grateful to Jaypee University of Engineering and Technology, Guna for providing financial asistance and Indian Institute of Technology, Roorkee for valuable support.

REFERENCES

1. Adhikary D P, MuhlhausH B, Dyskin A V.A numerical study of flexural buckling of foliated rock slopes. *Int. J.Numer. Anal. Meth. Geomech.*, 2001, *25:871-884.*
2. Amini M, Majdi A, Aydan O. Stability analysis and the stabilisation of flexural Toppling failure. *Rock mechanics Rock Eng*,2009, *42-751-78.2*
3. AroraV K, Strength and deformational Behaviour of jointed rocks, 1987, Ph. D Thesis, IIT Delhi, India.
4. Arora V K, Ramamurthy T. A Simple approach to predict unconfined compressive strength of jointed rock mass. Proc. of the Asian Regional Symposium on rock slopes. Pub. A A Balkema. Rotterdom, Neth. New Delhi, 1993, pp. 13 BN-90-5410-243
5. Bindlish A. Bearing capacity of strip footings on jointed rocks. PhD thesis, IIT Roorkee, India, 2007
6. Cavers D S. Simple methods to analyze buckling of rock slopes. *Rock Mechanics*, 1980, *14, 87-104.*
7. Hoek E. An empirical strength criterion and its use in designing slopes and tunnels in heavily jointed weathered rock. *Proc., 6th Southeast Asian Conf. on Soil Engineering*, Taipei, 111–158. 1980
8. Hoek, E. Strength of jointed rock masses. *Geotechnique*, 1983, 33-3, 187–223.
9. Hoek E, Brown E T, The Hoek-Brown failure criterion- a 1988 update. Proc. Of 15th Canadian Rock Mechanics Symposium. Rock Engineering for Underground Excavation, J.H. Curran eds. 1082-31-38
10. Hoek E, and BrownE T. Practical estimates of rock mass strength. *Int. J. Rock Mech. Min. Sci.*, 1997, 34-8, 1165–1186.
11. Hoek, E. *Practical rock engineering*, Ed., http:// www.rocscience.com/hoek/ Practical Rock Engineering.asp. 2000
12. Hoek E, Carranza-Torres C, and Corkum B. Hoek-Brown criterion-2002 edition. Proc. NARMS-TAC Conf. Toronto,2002,1,267-273
13. Hoek E, Marinos P, and Marinos V, Characterization and Engineering Properties of Tectonically Undisturbed but Lithologically varied sedimentary rock masses, *Int. J. Rock Mech. Min. Sci.* 2005, 42(2)277-285.
14. Imani M, Fahimifar A, Sharifzadeh M. Bearing failure modes of rock foundation with consideration of joint spacing. Scientia Iranica A 2012,19(6), 1411-1421
15. Ramamurthy T, Arora, V K. Strength prediction for jointed rocks in confined and unconfined states. *Int. J. Rock Mech. Min. Sci. Geomech. Abstr*, 1994, 31-1, 9–22.
16. Singh, M. Engineering behaviour of jointed model materials. PhD thesis, IIT, New Delhi, India. 1997
17. Singh, M, Rao KS. Ramamurthy T. Strength and deformational behaviour of a jointed rock mass. *Rock Mech. Rock En*,. 2002, 35-11, 45–64.
18. Singh M, Rao K S, Bearing Capacity of Shallow Foundations in Anisotropic Non-Hoek–Brown Rock Masses. J. Geotech. Geoenviron. Eng., 2005, 131:1014-1023.

APPENDICES

List of Symbols

B = Slope Width

E_i = Young's Modulus intact rock

Ej = Young's Modulus jointed rock mass

E_r = Ratio of moduli

I = Moment of inertia for a mass of slab

J_f = Joint Factor

J_n = Frequency of joints/ m in the direction of loading

K = 1.0 Pin jointed ends

L_b = Length of slope subjected to buckling

n = Joint inclination parameter

P_{cr} = Critical load in flexural buckling

r = Joint strength parameter

σ_{cj} = Uniaxial compressive strength of jointed rock mass

σ_{ci} = Strength of intact rock.

Φ_j = Friction angle along the joint plane.

θ = Joint Angle with the horizontal

α = Side Slope Angle